

# Coexistence of Rutile and Trirutile Phases in a Natural Tapiolite Sample

E. J. Kinast, L. I. Zawislak, J. B. M. da Cunha, V. Antonietti, M. A. Z. de Vasconcellos, and C. A. dos Santos<sup>1</sup>

*Instituto de Física, UFRGS, C.P. 15051, Campus do vale, 91501-970 Porto Alegre RS, Brazil*

Received July 3, 2001; in revised form August 29, 2001; accepted September 7, 2001

We report X-ray powder diffraction (XRD), electron probe microanalysis (EPMA), and Mössbauer spectroscopy (MS) measurements performed on a natural tapiolite with composition  $\text{Fe}_{0.57}\text{Mn}_{0.37}\text{Ti}_{0.10}\text{Ta}_{1.27}\text{Nb}_{0.67}\text{O}_6$ . XRD and MS suggest that besides being partially ordered the as-collected sample is a mixture of trirutile ( $P4_2/mnm$ ,  $a = 4.7532(9)$  Å,  $c = 9.228(7)$  Å) and Nb-rich rutile ( $P4_2/mnm$ ,  $a = 4.856(2)$  Å,  $c = 3.098(1)$  Å) structures. The Mössbauer spectra of the rutile (Fe, Mn, Ta, Nb) $\text{O}_2$  were fitted to  $\Delta = 1.72 \pm 0.05$  mm/s and  $\delta = 1.10 \pm 0.03$  mm/s at 300 K and to  $\Delta = 2.10 \pm 0.06$  mm/s and  $\delta = 1.18 \pm 0.03$  mm/s at 80 K. The present results suggest that cation ordering in compounds of the tapiolite series can be easily assessed by Mössbauer spectroscopy in a way similar to that as previously demonstrated for the columbite series. © 2002 Elsevier Science

**Key Words:** tapiolite; rutile; trirutile; order–disorder; oxidation; Mössbauer spectroscopy; X-ray diffraction; electron probe microanalysis.

## 1. INTRODUCTION

The  $AB_2O_6$  family of compounds encompasses two different solid solutions. One, orthorhombic, is named tantalite-columbite and the other one, tetragonal, is named tapiolite (1–4). In terms of natural occurrences the most relevant chemical composition is that for which  $A = \text{Fe, Mn}$ , and  $B = \text{Ta, Nb}$ , with minor substitutions of Sn, W, and Ti. However, isomorphous compounds can be prepared with  $A = \text{Ni, Co, Cu, Zn}$  (5–7) and  $B = \text{Sb}$  (8). Besides their economic importance (they are the major source of tantalum) these materials present interesting physical properties which have motivated the investigations reported in the past two decades.

As illustrated in Fig. 1, ordered  $AB_2O_6$  crystallizes with the trirutile structure in space group  $P4_2/mnm$ , with  $\text{Fe}^{2+}$  (site  $A$ ) and  $\text{Ta}^{5+}$  (site  $B$ ) cations surrounded by  $\text{O}^{2-}$

octahedra, and successive Fe–O planes (at  $z = 0$  and  $z = \frac{1}{2}$ ) separated by two Ta–O planes (at  $z = \frac{1}{6}$  and  $z = \frac{1}{3}$ ). Random distribution of  $A$  and  $B$  cations result in the disordered rutile structure ( $MO_2$ ), as indicated by the smallest unit cell in Fig. 1. Therefore, as for the orthorhombic series (9–11), the tetragonal one presents an order–disorder transition and  $(\text{Fe, Mn, Ta, Nb})\text{O}_2$  transforms into  $(\text{Fe, Mn})(\text{Ta, Nb})_2\text{O}_6$  as a consequence of cation ordering. Usually the investigation of this kind of phenomena has been performed using X-ray diffraction (XRD). However, for several samples it is difficult to distinguish the disordered structure from one partially ordered by measuring their supercell reflections, even when analysis is done by complex and time-consuming procedures based on Rietveld refinement (10).

Wise and Cerný (4) pointed out that the attempt to quantify the degree of order by using XRD measurements has proven to be unsatisfactory because the supercell reflections are also strongly dependent on the Mn and Ti contents. Therefore, according to these authors, a quick and simple means of determining the degree of order in this kind of material is not yet available. Recently it has been demonstrated that Mössbauer spectroscopy (MS) is a very efficient tool to investigate order–disorder phenomena in the orthorhombic series (9, 12, 13). As long as hyperfine interactions are very sensitive to change of the near-nearest environment, MS enables us to easily differentiate  $^{57}\text{Fe}$  on the  $A$  site from  $^{57}\text{Fe}$  on the  $B$  site.

In the present paper we report cation ordering and oxidation reaction on a quite peculiar tapiolite sample, showing the coexistence of rutile and trirutile structures. The cation order parameter proposed by Augsburger *et al.* (13) for columbite samples will be used here to quantify the cation order percentage.

## 2. EXPERIMENTAL DETAILS

The sample is a crystal of tapiolite collected from the Borborema pegmatite, in the Paraíba State, northeast of

<sup>1</sup>To whom correspondence should be addressed. Fax: + (55 51) 33 16 72 86. E-mail: [cas@if.ufrgs.br](mailto:cas@if.ufrgs.br).

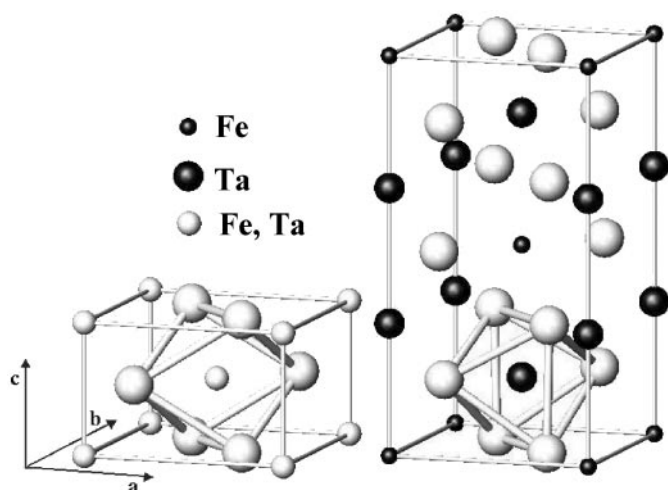


FIG. 1. Schematic representations of the  $\text{FeTa}_2\text{O}_6$  (trirutile) and  $(\text{Fe,Ta})\text{O}_2$  (rutile) structures. The oxygen atoms are represented by the biggest spheres.

Brazil (14). The chemical composition from electron probe microanalysis is approximately  $\text{Fe}_{0.57}\text{Mn}_{0.37}\text{Ti}_{0.10}\text{Ta}_{1.27}\text{Nb}_{0.67}\text{O}_6$ , hereafter simply  $(\text{Fe, Mn})(\text{Ta, Nb})_2\text{O}_6$ . A crystal fragment was powdered and submitted to two heat treatments: one part was heated in air, while the other one was heated in vacuum ( $P \cong 10^{-5}$  Pa). In order to compare with published results (1, 4, 9, 11, 12), all the samples were heated at 1320 K for 48 h and subsequently slowly cooled at 15 K/h. This cooling rate is adequate for cation ordering, e.g., all Fe + Mn in site A and all Ta + Nb in site B of the orthorhombic and tetragonal  $\text{AB}_2\text{O}_6$  structures.

Electron probe microanalyses (EPMA) were performed on the as-collected sample with a wavelength dispersive (WDS) microprobe system (CAMECA SX50). An accelerating potential of 15 kV, a beam current of 25 nA, and a beam size of approximately  $1 \mu\text{m}$  were used. Pure Nb ( $\text{Nb } L\alpha$ ), pure Ta ( $\text{Ta } L\alpha$ ), synthetic rutile ( $\text{Ti } K\alpha$ ), natural olivine ( $\text{Mn } K\alpha$ – $\text{Fe } K\alpha$ ), and pure W ( $\text{W } L\alpha$ ) were used as standards. The counting time was 20 s for Nb and Ta and 30 s for the remaining elements. The raw data were corrected on-line for drift, deadtime, and background using PAP correction programs. The formula was calculated on the basis of six O atoms, and taken from 20 analyses.

XRD patterns were obtained in Bragg–Brentano geometry by means of a Siemens diffractometer D500, equipped with a curved graphite monochromator and  $\text{Cu } K\alpha$  radiation ( $\text{Cu } K\alpha_1 = 1.5406 \text{ \AA}$ ,  $\text{Cu } K\alpha_2 = 1.5444 \text{ \AA}$ ) and calibrated with polycrystalline Si. Measurements were performed with a scan step of  $0.05^\circ 2\theta$  in the  $2\theta$  range from  $10^\circ$  to  $120^\circ$ , with a fixed counting time of 1 s. The profile parameters were obtained using a model-independent fitting with the program FullProf (15). Starting unit cell parameters were taken from JCPDS files 23-1124 (tapiolite), 16-0934 (rutile), 43-0798 ( $\text{Fe TaO}_4$ ), and 25-0922 ( $\text{Ta}_2\text{O}_5$ ) (16).

Absorbers for the MS measurements were prepared with appropriate amounts of ground (320 mesh) material in order to satisfy the ideal absorber thickness approximation (17). The spectra were taken at 300 and 80 K, using a constant acceleration electromechanical drive system with a multi-channel analyzer for collecting and storing the data. The velocity scale was calibrated using a high-purity Fe foil. The hyperfine parameters were obtained by a least-squares procedure assuming Lorentzian line shapes constrained to equal half-widths.  $^{57}\text{Co}$  in rhodium was used at room temperature as a source, with nominal activity of 25 mCi. Isomer shift data are relative to  $\alpha$ -Fe. Typical errors are  $\pm 3\%$  on hyperfine parameters and  $\pm 5\%$  on site occupancies.

### 3. RESULTS AND DISCUSSION

Figure 2a shows the XRD pattern for the as-collected sample. It was indexed to two phases, both belonging to the space group  $P4_2/mnm$ . The one with more intense reflections exhibits lattice parameters (see Table 1) typical of tapiolite,  $(\text{Fe, Mn})(\text{Ta, Nb})_2\text{O}_6$  (3, 4, 6, 8), while the one with low-intensity reflections shows lattice parameters similar to

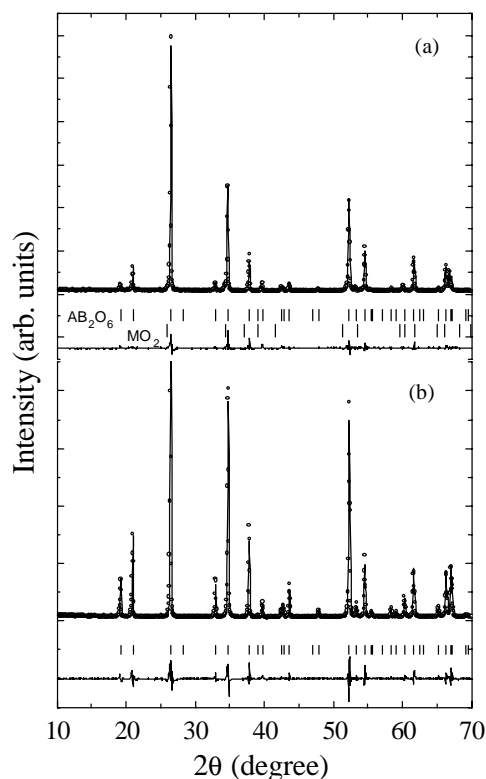


FIG. 2. Representative parts of the X-ray powder diffraction patterns for (a) as-collected sample and (b) heated-in-vacuum sample. The open circles represent observed data. The solid line represents the calculated pattern obtained with the Rietveld refinement. The lower trace is a plot of the residual spectrum, observed minus calculated intensities.

**TABLE 1**  
Unit Cell Parameters Obtained in the Present Work

Sample	Phase	Space group	$a$ (Å)	$b$ (Å)	$c$ (Å)	$R_{wp}$
As-collected	Tapiolite	$P4_2/mnm$	4.7532(9)	4.7532(9)	9.228(7)	11.2
	(Fe, Mn, Ta, Nb) $O_2$	$P4_2/mnm$	4.856(2)	4.856(2)	3.098(1)	
Heated-in-vacuum	Tapiolite	$P4_2/mnm$	4.7245(6)	4.7245(6)	9.198(5)	10.9
Heated-in-air	(Fe, Mn)(Ta, Nb) $O_4$	$P4_2/mnm$	4.690(1)	4.690(1)	3.052(7)	12.1
	(Ta, Nb) $_2O_5$	$C2mm$	6.213(3)	40.200(3)	3.889(2)	

Note. Numbers in parentheses designate  $\pm 1\sigma$  on the last decimal given.  $R_{wp} = 100 \{ \sum_i w_i [y_i(\text{obs}) - y_i(\text{calc})]^2 / \sum_i w_i [y_i(\text{obs})]^2 \}^{1/2}$ .

those reported for the compound (Fe, Mn, Ta, Nb) $O_2$ , with the rutile structure (1). As discussed below, from MS measurements the rutile phase accounts for less than 10%. Figure 2b displays the XRD pattern for the heated-in-vacuum sample. It was indexed to a single phase with lattice parameters typical of tapiolite, but with the  $c$  parameter slightly smaller as compared to that of the as-collected sample, which is indicative of ordering (11). In addition, the supercell reflections (at  $2\theta = 19.28, 21.03, 32.99, 43.69$ , and  $55.55$ ) are more intense in Fig. 2b. Therefore, it is evident that cation ordering has been provided by the in-vacuum heat treatment. To be specific, the disordered (Fe, Mn, Ta, Nb) $O_2$  compound transforms into ordered (Fe, Mn)(Ta, Nb) $_2O_6$  and the partially ordered (Fe, Mn)(Ta, Nb) $_2O_6$  compound transforms into a completely ordered one. However, there is no quantitative criterion to fully evaluate this ordered state, such as the one established by Ercit's equation for columbite (11). Therefore, our X-ray-based evaluation of the order-disorder transformation should be limited to a qualitative account.

In Fig. 3 we display the room-temperature MS spectra for the samples whose XRD patterns are shown in Fig. 2. The spectrum for the as-collected sample was fitted to three doublets (see Table 2), all attributed to high-spin  $Fe^{2+}$  in octahedral coordination. The doublet with  $\Delta = 3.04 \pm 0.09$  mm/s is typical of tapiolite (18, 19). The doublet with the smallest quadrupole splitting ( $\Delta = 1.72 \pm 0.05$  mm/s) is in the range of those attributed to columbite (orthorhombic (Fe, Mn)(Ta, Nb) $_2O_6$ ) (10–13), whereas the intermediate doublet ( $\Delta = 2.48 \pm 0.07$  mm/s) has not been reported for compounds of these families. Following the reasoning presented for partially ordered columbite samples (10–13), we can attribute the doublet  $\Delta = 2.48 \pm 0.07$  mm/s to  $^{57}Fe$  in the  $B$  site of the tetragonal  $AB_2O_6$  structure; doing so means  $^{57}Fe$  substituting for Ta in the  $TaO_6$  octahedra. Therefore, the partially ordered (Fe, Mn)(Ta, Nb) $_2O_6$  tapiolite is characterized by two doublets: one ( $\Delta = 3.04 \pm 0.09$  mm/s) attributed to  $^{57}Fe$  in the  $FeO_6$  octahedra and the other one ( $\Delta = 2.48 \pm 0.07$  mm/s) attributed to  $^{57}Fe$  in the  $TaO_6$  octahedra.

The smallest quadrupole splitting ( $\Delta = 1.72 \pm 0.05$  mm/s), contributing 9% to the total spectral area, could be attributed to somewhat disordered orthorhombic (Fe, Mn)(Ta, Nb) $_2O_6$  (10–13). However, the XRD patterns for both as-collected and heated-in-vacuum samples enable us to reject this conjecture. There is no signal of orthorhombic phase in these patterns. Felten (20) showed that for the related systems  $CoTa_2O_6$ – $CoNb_2O_6$  and  $NiTa_2O_6$ – $NiNb_2O_6$ , the Nb-rich samples crystallize with the rutile

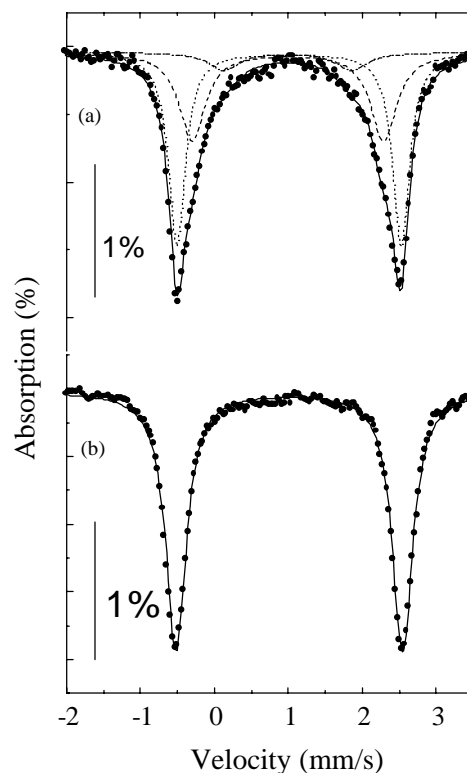


**FIG. 3.** Mössbauer spectra taken at 300 K for (a) as-collected sample and (b) heated-in-vacuum sample. The circles represent observed data. The solid lines represent the calculated spectra based on a least-squares procedure. Dashed lines represent the calculated subspectra.

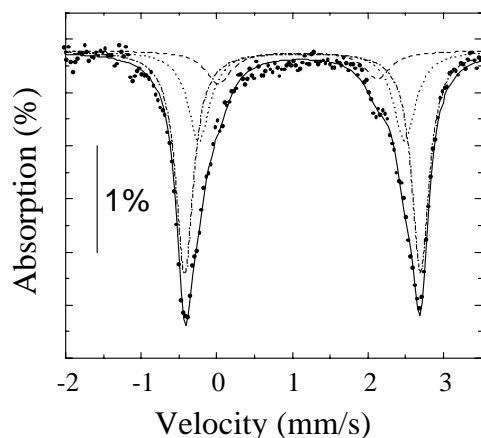


FIG. 4. The same as in Fig. 3, for measurements taken at 80 K.

structure, while the Ta-rich ones exhibit the trirutile structure. Keeping in mind the XRD results and the similarity between those samples and the present one, we have attributed  $\Delta = 1.72 \pm 0.05$  mm/s to a disordered Nb-rich rutile structure of the type  $(\text{Fe, Mn, Ta, Nb})\text{O}_2$ . The back-scattered electron images show heterogeneous cation distributions, suggesting the possibility of a local high Nb density. In such a region, rutile structure instead of trirutile could crystallize.

To the best of our knowledge there is no Mössbauer measurement reported for the rutile structure  $(\text{Fe, Mn, Ta, Nb})\text{O}_2$ . However, our conjecture can be evaluated by performing Mössbauer measurements at 80 K, as shown in Fig. 4 and Table 2. From the relative spectral areas the following correspondences can be stated for  $\Delta$  at 300 and 80 K:  $3.04 \rightarrow 3.11$  mm/s,  $2.58 \rightarrow 2.72$  mm/s, and  $1.72 \rightarrow 2.10$  mm/s. Thus, the larger quadrupole splitting is almost temperature independent, as expected for ordered

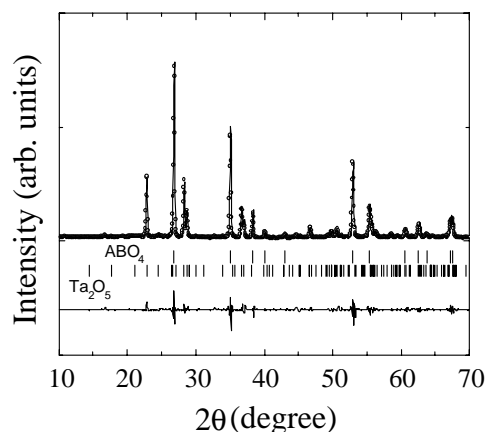


FIG. 5. Representative part of the X-ray powder diffraction pattern for the heated-in-air sample. The open circles represent observed data. The solid line represents the calculated pattern obtained with the Rietveld refinement. The lower trace is a plot of the residual spectrum, observed minus calculated intensities.

$\text{FeTa}_2\text{O}_6$  (21). In addition, the temperature dependence is more significant as the quadrupole splitting decreases, or, from the ordered to the disordered component. This result is very similar to that reported for the series  $\text{FeTaO}_4$ – $\text{FeTa}_2\text{O}_6$  (22), for which the strong temperature dependence of  $\Delta$  observed in some samples was attributed to a locally disordered structure.

Our hypothesis can also be examined by looking for the effect of oxidation on the as-collected sample. In Fig. 5 we show the XRD pattern for the heated-in-air sample. It was indexed (see Table 1) to a mixture of tetragonal  $(\text{Fe, Mn})(\text{Ta, Nb})\text{O}_4$  (rutile structure) and orthorhombic  $(\text{Ta, Nb})_2\text{O}_5$ . The presence of  $(\text{Fe, Mn})(\text{Ta, Nb})\text{O}_4$  has been confirmed by MS measurement, as can be seen in Fig. 6 and Table 2. The obtained hyperfine parameters

TABLE 2  
Hyperfine Parameters for All Measurements Reported in the Present Work

Sample	Compound	Site assignment	$\Delta$ (mm/s)	$\delta$ (mm/s)	$\Gamma$ (mm/s)	$A$ (%)
As-collected, Meas. at 300 K	Tapiolite	$\text{FeO}_6$	3.04	1.12	0.27	56
		$\text{TaO}_6$	2.58	1.10	0.41	35
		$(\text{Fe, Mn, Ta, Nb})\text{O}_2$	1.72	1.10	0.50	9
As-collected, Meas. at 8 K	Tapiolite	$\text{FeO}_6$	3.11	1.24	0.29	59
		$\text{TaO}_6$	2.72	1.23	0.39	32
		$(\text{Fe, Mn, Ta, Nb})\text{O}_2$	2.10	1.18	0.40	9
Heated-in-vacuum	Tapiolite	$\text{FeO}_6$	3.06	1.12	0.33	100
Heated-in-air	$(\text{Fe, Mn})(\text{Ta, Nb})\text{O}_4$	$\text{FeO}_6$	0.52	0.41	0.34	100

Note.  $\Delta$  is the quadrupole splitting at the iron sites;  $\delta$  is the isomer shift relative to  $\alpha$ -Fe;  $\Gamma$  is the linewidth at half-height;  $A$  is the site occupancy, given by the relative spectral area. Typical errors are  $\pm 3\%$  on hyperfine parameters and  $\pm 5\%$  on site occupancies.

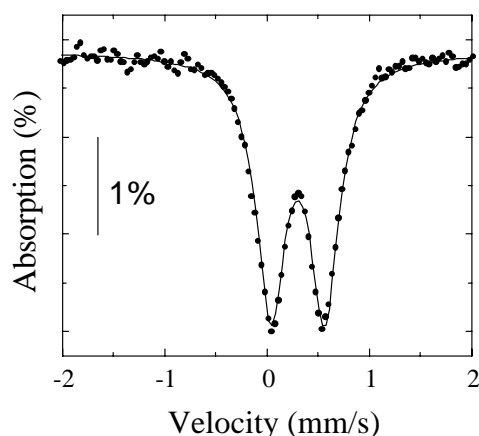


FIG. 6. Mössbauer spectrum taken at 300 K for the heated-in-air sample. The circles represent observed data. The solid line represents the calculated spectra based on a least-squares procedure.

( $\Delta = 0.52$  mm/s,  $\delta = 0.41$  mm/s) are quite similar to those attributed to synthetic  $\text{FeTaO}_4$  ( $\Delta = 0.53$  mm/s,  $\delta = 0.43$  mm/s) (23). Therefore, the fact that oxidation of the as-collected sample produced tetragonal  $(\text{Fe, Mn})(\text{Ta, Nb})\text{O}_4$  supports our choice in attributing  $\Delta = 1.72 \pm 0.05$  mm/s to the tetragonal  $(\text{Fe, Mn, Ta, Nb})\text{O}_2$  compound.

Thus, the as-collected sample is a mixture of disordered rutile and partially ordered trirutile compounds. Cation ordering induced by heating in vacuum is clearly observed by XRD and MS measurements. Also, the effect of oxidation, by heating in air, is consistently displayed by XRD and MS. For the as-collected sample, 56% of the  $^{57}\text{Fe}$  atoms are in the *A* site of the trirutile structure, 35% are in the *B* site, and 9% are in the rutile structure. The problem is how to assess the degree of cation order. For columbite samples, there is Ercit's formula (11) based on the *a* and *c* unit cell parameters and a Mössbauer-based parameter recently proposed by Augsburgberger *et al.* (13),

$$x(\%) = -50 + 1.515A_A,$$

where  $A_A$  is the relative spectral area attributed to the *A* site of the  $\text{AB}_2\text{O}_6$  structure.

Unfortunately, there is no quantitative criterion to assess the degree of cation order from XRD measurements for tapiolite samples. For MS measurements we can use the *x* parameter given above. Normalizing the relative spectral areas for the trirutile structure (62% of the  $^{57}\text{Fe}$  atoms in the *A* site and 38% in the *B* site), we obtain 44% for the cation order percentage. However, at this moment such a criterion is only a suggestion and should be compared to the degree of cation order obtained by other techniques and methods to be firmly accepted.

#### 4. CONCLUSIONS

We have reported XRD, EPMA, and MS measurements performed on a natural sample containing a partially ordered tapiolite with composition  $\text{Fe}_{0.57}\text{Mn}_{0.37}\text{Ti}_{0.10}\text{Ta}_{1.27}\text{Nb}_{0.67}\text{O}_6$  and a rutile phase probably with composition  $(\text{Fe, Mn, Ta, Nb})\text{O}_2$ . Heating in vacuum promotes the ordering of both phases. That is to say, the tapiolite becomes completely ordered and  $(\text{Fe, Mn, Ta, Nb})\text{O}_2$  transforms into  $(\text{Fe, Mn})(\text{Ta, Nb})_2\text{O}_6$ . The present results suggest that cation ordering in compounds of the tapiolite series can be easily assessed by Mössbauer spectroscopy in a way similar to that demonstrated for the columbite series. It is obvious that MS probes exclusively  $^{57}\text{Fe}$  cation ordering. However, assuming equal *f*-factors for both sites of the trirutile structure (supported by the MS measurements at 80 K) and the same probability for site occupancy of both Fe and Mn, Augsburgberger *et al.* (13) were able to propose the cation order degree parameters given above for columbite samples, which can also be used for tapiolite ones.

#### ACKNOWLEDGMENTS

We thank Dr. M. Adusumilli (UNB, Brazil) for providing us with the sample used in this work. We are in debt to Dr. P. M. Mors and Prof. F. C. Zawislak for critical reading of the manuscript. This work was supported in part by the Brazilian agencies CAPES and CNPq.

#### REFERENCES

1. C. Hutton, *Am. Mineral.* **43**, 112 (1958).
2. E. H. Nickel, J. F. Rowland, and R. C. McAdam, *Can. Mineral.* **7**, 390 (1963).
3. A. C. Turnock, *Can. Mineral.* **8**, 461 (1966).
4. M. A. Wise and P. Cerný, *Can. Mineral.* **34**, 631 (1996).
5. C. Heid, H. Weitzel, F. Bourdarot, R. Calenczuk, T. Vogt, and H. Fuess, *J. Phys.: Condens. Matter.* **8**, 10609 (1996).
6. V. Antonietti, E. J. Kinast, L. I. Zawislak, J. B. M. da Cunha, and C. A. dos Santos, *J. Phys. Chem. Solids* **62**, 1239 (2001).
7. J. Norwig, H. Weitzel, H. Paulus, G. Lautenschläger, J. Rodriguez-Carvajal, and H. Fuess, *J. Solid State Chem.* **115**, 476 (1995).
8. J. N. Reimers, J. E. Greedan, C. V. Stager, and R. Kremer, *J. Solid State Chem.* **83**, 20 (1989).
9. L. I. Zawislak, V. Antonietti, J. B. M. da Cunha, and C. A. dos Santos, *Solid State Commun.* **101**, 767 (1997).
10. M. Wenger, T. Armbruster, and C. A. Geiger, *Am. Mineral.* **76**, 1897 (1991).
11. T. S. Ercit, M. A. Wise, and P. Cerný, *Am. Mineral.* **80**, 613 (1995).
12. C. A. dos Santos, L. I. Zawislak, V. Antonietti, E. J. Kinast, and J. B. M. da Cunha, *J. Phys.: Condens. Matter.* **11**, 7021 (1999).
13. M. S. Augsburgberger, J. C. Pedregosa, G. M. Sosa, and R. C. Mercader, *J. Solid State Chem.* **143**, 219 (1999).
14. M. S. Adusumilli, Ph.D. Thesis, Universidade Federal de Minas Gerais, Brazil (in Portuguese), 1976.
15. J. Rodriguez-Carvajal, *Physica B* **192**, 55 (1993).
16. Joint Committee on Powder Diffraction Standards, published by International Centre for Diffraction Data, Swarthmore, PA, 1995.
17. G. J. Long, T. E. Cranshaw, and G. Longworth, *Mössbauer Eff. Ref. Data J.* **6**, 42 (1983).

18. S. M. Eicher, J. E. Greedan, and K. J. Lushington, *J. Solid State Chem.* **62**, 220 (1986).
19. L. I. Zawislak, G. L. F. Fraga, J. B. Marimona da Cunha, D. Schmitt, A. S. Carriço, and C. A. dos Santos, *J. Phys.: Condens. Matter.* **9**, 2295 (1997).
20. E. J. Felten, *Mater. Res. Bull.* **2**, 13 (1967).
21. C. A. dos Santos and J. de Oliveira, *Solid State Commun.* **82**, 89 (1992).
22. E. Schmidbauer and J. Lebkuchner-Neugebauer, *Phys. Chem. Miner.* **15**, 196 (1987).
23. D. N. Astrov, N. A. Kryukova, R. B. Zorin, V. A. Makarov, R. P. Ozerov, F. A. Rozhdestvenskii, V. P. Smirnov, A. M. Turchaninov, and N. V. Fadeeva, *Sov. Phys.-Cryst.* **17**, 1017 (1973).